Calcif. Tissue Int. 33, 631–639 (1981)

Calcified Tissue International

Radiographic Evidence of Disuse Osteoporosis in the Monkey (*M. nemestrina*)

D. R. Young and V. S. Schneider

Biomedical Research Division, Ames Research Center, NASA, Moffett Field, California 94035, USA; and Department of Health, Education and Welfare, Public Health Service Hospital, San Francisco, California 94118, USA

Summary. Radiological techniques were utilized for monitoring progressive changes in compact bone in the tibia of monkeys during experimentally induced osteopenia. Bone mass loss in the tibia during restraint was evaluated from radiographs, from bone mineral analysis, and from images reconstructed from gamma ray computerized tomography. The losses during 6 months of restraint tended to occur predominantly in the proximal tibia and were characterized by subperiosteal bone loss, intracortical striations, and scalloped endosteal surfaces. Bone mineral content in the cross section of the tibia declined 17–21%. Tomography demonstrated endosteal widening and reduced mineral content per unit of thickness of cortical bone. In 6 months of recovery, the mineral content of the proximal tibia remained depressed. Effects of the dynamic environment on local-regional changes in various skeletal areas are discussed.

Key words: Bone — Osteopenia — Noninvasive monitoring.

There is ample evidence that skeletal mass is regulated by mechanical factors. Reduction of skeletal loading through bed rest results in an increased urinary and fecal calcium output [1, 2]. The loss of bone in humans confined to bed for long periods is well known [2, 3]. By contrast, other tests show the positive effects of skeletal stressing. Bipedal rats (without forelimbs) develop more muscle and stronger bones in the hind limbs than quadrupedal controls [4], and dogs with resected radii show a marked adaptive hypertrophy of the ulnae [5]. Also, exercise such as tennis [6] produces an increase of humeral bone mass. Apparently, the stress state in proximity to bone surfaces regulates adaptive remodeling.

In recent years, the restrained primate has been studied to develop a useful model for the evaluation of disuse osteoporosis. Kazarian and von Gierke [7] demonstrated that 60 days of immobilization of monkeys had a dramatic effect on cancellous bone; a reduction of compressive strength of the lumbar vertebrae by a factor of 2 to 3 was noted. Young et al. [8, 9] evaluated changes in the appendicular skeleton of restrained monkeys and demonstrated the lability of tibial bone mineral content, this in sharp contrast to the stable radius and ulna. There appeared to be local rather than diffuse rarefying atrophy in the tibia, suggesting the possibility of increased sensitivity of local areas in the proximal tibia to resorptive factors during restraint.

Regional bone mass loss that possibly may involve a relatively small portion of the skeletal system is difficult to evaluate from the standpoint of obtaining optimal information regarding skeletal changes. In the present series, studies were conducted with a few restrained monkeys in order to develop preliminary comparisons between three noninvasive radiological techniques used to monitor adaptive remodeling and, in particular, to assess the osteopenia arising from excessive bone resorption. The techniques involved X-rays, photon absorptiometry, and gamma ray computer tomography. Tomography, applied to the appendicular skeleton, is a relatively new approach for evaluating cortical thinning and endosteal widening.

Materials and Methods

Experiments were conducted with 3 adult, male, pigtail (*Macaca nemestrina*) monkeys; body weight of the monkeys ranged from 10 to 14 kg. The animals were maintained on lab chow (Purina). Two animals were restrained according to the tech-

Send offprint requests to D. R. Young at the above address.

0171-967X/81/0033-0631 $01.80

nique of Howard et al. [10] in order to minimize stress loading in the lower extremities. The animals were maintained in a semi-reclined position (40° above horizontal) with the lower legs resting on a foot rest. This type of immobilization reduces normally occurring stresses in the lumbar vertebrae, pelvis, and legs. The third animal served as the nonrestrained control. The experiment consisted of 6 months of stabilization in metabolic cages, followed by 6 months of restraint, followed by 7 months of recovery and rehabilitation; the latter period included sessions of daily treadmill walking.

Tibial bone mass and mineral content were evaluated as follows:

1. X-rays were taken with a soft beam utilizing Kodak AA slow-speed industrial-type film in order to produce a relatively high resolution image.

2. Mineral content was measured with the Norland-Cameron Model 178 Bone Mineral Analyzer. The measurement is based on the attenuation of photon flux from a ^{125}I source. The probability of photoelectric adsorption per unit mass varies as the cube of the atomic number; therefore, it is much more likely in calcium and phosphorus than in carbon, oxygen, or nitrogen. Transverse scans of bones provide an integrated value of bone mineral content in the cross section. Measurements were made in the tibia, 2.8 cm below the distal femur and in the proximal, distal, and midshaft of the diaphysis of the radius and ulna. Measurement precision is 3%.

3. Visual displays of the cross section were obtained with an ISOTOM, a precision scanning instrument described by Rüegsegger et al. [11, 12] for the determination of mineral distribution in bone. During each scan of the proximal tibia, photon flux from a ^{125}I source is determined for 128 equal intervals of time. After each linear scan, the gamma beam and the detector are rotated 3.0° until the procedure has been carried out through 180° of rotation. A shadograph of the cross section is reconstructed with 128 × 128 individual matrix cells (pixels); the absorption coefficients for the individual cells, based on mineral distribution, are computed. In the mathematical model [12], the ratio of the linear absorption coefficients of soft tissue, compact bone, and trabecular bone is 1:8:2. The mineral distribution per unit thickness of the cross section is visualized by assigning different colors to the matrix cells according to the magnitude of the absorption coefficients; the reconstructed image is displayed on a screen. Limb repositioning studies were performed with each animal to gain a measure of the precision of the data. In replicate trials, computed cross-sectional areas of bone measured at a particular site usually agreed within 1% or better. The largest difference was 6%.

Results

Figure 1 is a print of a radiograph from the control animal. Dense, thick cortical bone in the anterior tibia begins approximately at the tibial tuberosity, 2 cm below the distal femur, and extends to the distal tibia. Figure 2A was taken from a radiograph of an experimental animal just prior to restraint. The anterior cortex is smooth, without striations. Figure 2B shows the response to 2½ months of restraint. There is a loss of cortical bone in the anterior tibia approximately 2.8 cm below the distal femur. There are resorption cavities at the endosteal surface with an apparent splitting of the inner cortex, and there

Fig. 1. Print of a radiograph of the left tibia of control animal No. 27. All X-rays were taken of the mediolateral aspect. There is heavy cortical bone in the anterior and posterior tibia. Trabecular bone is prominent in the proximal and distal tibia

are occasional striations in the anterior cortex. Figure 2C shows the response to 5 months of restraint. There are further losses of cortical bone in the anterior tibia and well-defined cortical striations. There is also surface erosion in the proximal tibia; it extends to the juxta-articular area with a resulting accentuation of the patterns of the underlying bone architecture. Figure 2D, taken at 1 month of recovery, is generally similar to the pattern seen at the end of restraint. Figure 2E, taken at 6 months of recovery, continues to show a well-defined cortical striation. There has been some replacement of the bone in the cortex below the tibial tuberosity.

Figure 3A shows the tibia of a second experimental animal prior to restraint. Figure 3B shows intracortical striations in the anterior proximal tibia after 2½ months of restraint. Figure 3C, taken at 5 months of restraint, shows loss of cortical bone in the anterior proximal tibia with an apparent splitting of the inner cortex. There are numerous intracortical striations in the anterior tibia; there is also surface erosion. Figure 3D shows the continued losses in 1 month of recovery. Intracortical resorption spaces appear in the midshaft and distal tibia. There has been progressive enlargement of the medullary canal in the proximal fibula. Figure 3E, taken after 6 months of recovery, shows restoration of cortical

Fig. 2. A Left tibia of animal BO_9 prior to restraint. B Tibia of BO_9 after 2½ months of restraint. Note subperiosteal bone loss in the anterior proximal tibia, resorption cavities at the endosteal surface, and occasional intracortical striations. C After 5 months of restraint there is erosion of surface bone in the proximal tibia with an apparent accentuation of the underlying bone architecture. There is a well-defined intracortical striation in the anterior tibia. D In 1 month of recovery, the pattern is similar to that observed in the last month of restraint. E After 6 months of recovery there has been restoration of intracortical and subperiosteal bone in the anterior proximal tibia

bone in the anterior proximal tibia and a reduction in the number of intracortical striations.

Figure 4 shows the bone mineral measurements in the proximal left tibia, 2.8 cm below the distal femur. There is a 17–21% decline of bone mineral content within 5 months of restraint. Test animal BO_3 shows initially a further significant decline in 1 month of recovery and then a gradual increase of mineral content. Animal BO_9 did not show improvement during recovery. The control animal showed only random variations during the 1-year period of observation.

Although there was an increased radiographic density seen during recovery, the radiographic contrast in the anterior tibia is considerably less than that seen in the posterior tibia, indicating the presence of resorption cavities and less bone per unit thickness of cortex. The degree of improvement was not reflected in a distinctive rise of bone mineral in the entire cross section.

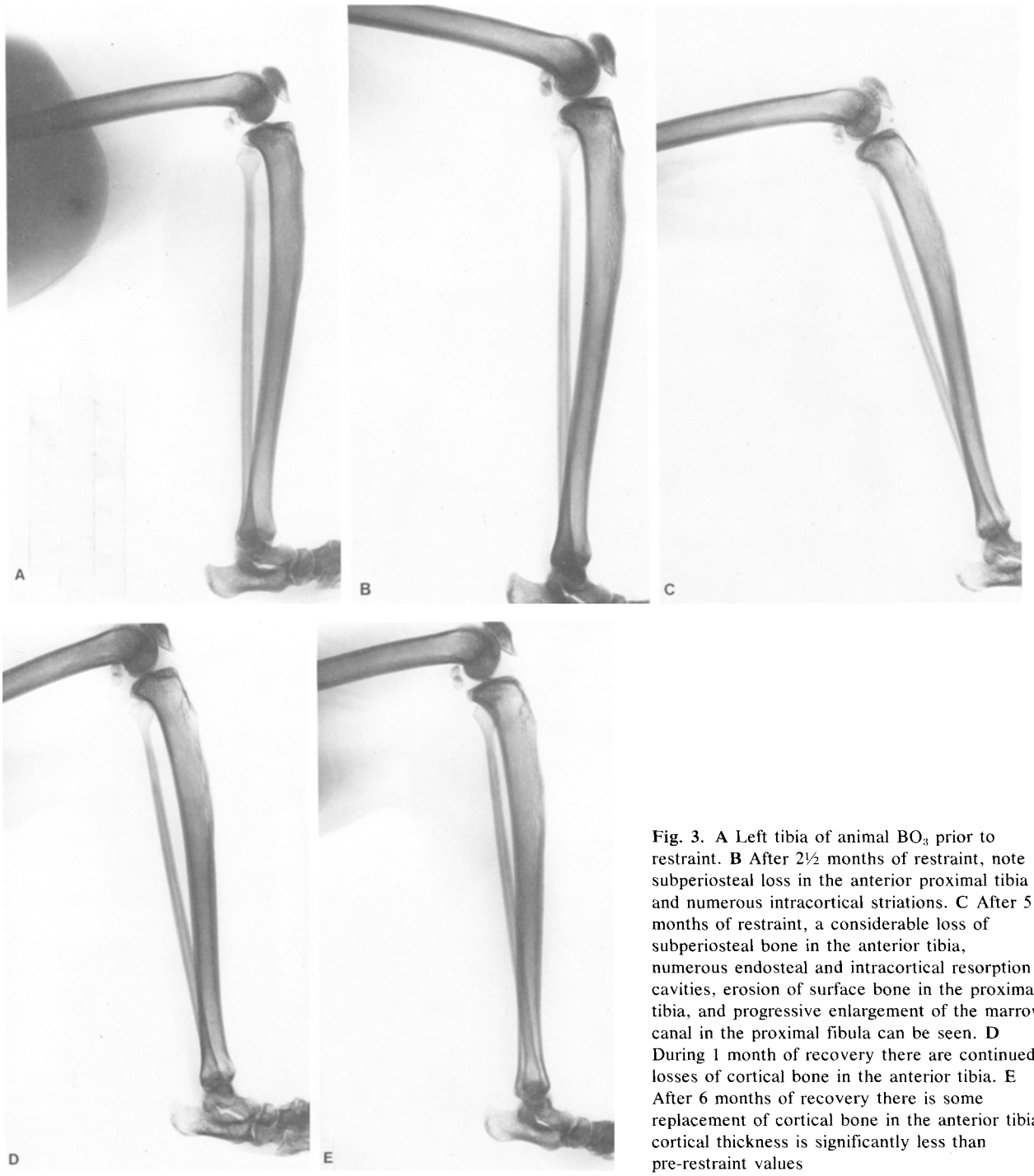

Fig. 3. A Left tibia of animal BO_3 prior to restraint. B After 2½ months of restraint, note subperiosteal loss in the anterior proximal tibia and numerous intracortical striations. C After 5 months of restraint, a considerable loss of subperiosteal bone in the anterior tibia, numerous endosteal and intracortical resorption cavities, erosion of surface bone in the proximal tibia, and progressive enlargement of the marrow canal in the proximal fibula can be seen. D During 1 month of recovery there are continued losses of cortical bone in the anterior tibia. E After 6 months of recovery there is some replacement of cortical bone in the anterior tibia; cortical thickness is significantly less than pre-restraint values

Tomograms of the proximal tibia were taken at various phases of testing. Unfortunately, an instrumentation failure made baseline scans impossible. Figure 5a–c shows the reconstruction for the control animal. There is heavy mineralized bone distributed throughout the cortex. Figure 6A shows the proximal tibia of animal BO_3 after 5 months of restraint. There is relatively little dense mineralized bone in the anterior tibia. Figure 6B, taken after 4 months of recovery, shows a relative deficiency of mineralized bone in the anterior tibia.

Interpretation of the color coding for the individual pixels in the restrained animal is as follows: increased erosion of bone leads to intracortical stri-

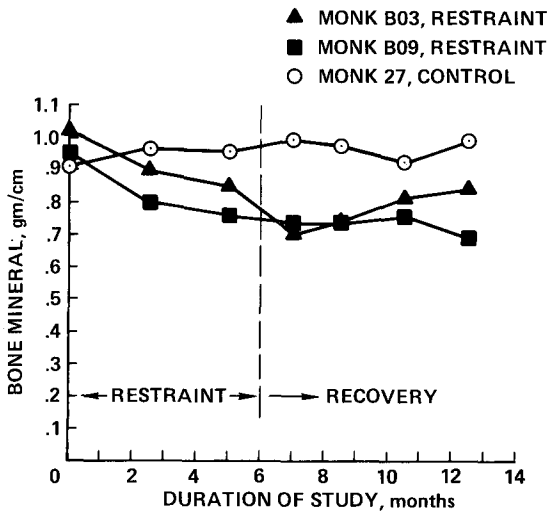

Fig. 4. Bone mineral content in the proximal tibia of monkeys. Mineral content in g/cm is shown on the vertical scale; duration of test in months is shown on the horizontal scale. Control animal is shown by open symbols (○). Restrained animals are shown by closed symbols (■; ▲)

ations, increased cortical porosity, and less bone mineral per unit thickness of bone (blue represents greatest mineral content; green, yellow, and red represent lesser mineral content).

Radiographs of the radius and ulna showed no changes, and bone mineral scans at various sites in the proximal, midshaft, and distal diaphysis were relatively constant. During the 1 year of observation, the range of ulnar midshaft mineral measurements of animal BO_9 varied from 0.31 to 0.32 g/cm; for animal BO_3 the range was 0.31–0.34 g/cm; and for No. 27 the corresponding range was 0.43–0.45 g/cm. Similar consistency was observed in the midshaft of the radius. For each animal, the average variability of forearm measurements was within the 3% reproducibility of the method.

Discussion

The present studies further document the time history of disuse osteoporosis in the monkey, particularly in regard to loss of cortical bone. Radiological techniques were utilized for the diagnosis and monitoring of progressive changes. The demonstration of slow recovery post-immobilization agrees generally with the photon absorptiometry data of Andersson and Nilson [13], who reported a 17% loss of bone mineral in the proximal tibia of patients with knee injuries treated with a plaster cast; there was no sign of restoration of bone mineral content in the tibia within the first year.

In our investigations, lack of weight bearing and exercise were the principal variables studied. In a prior report we examined the compressive strain-stress history in the tibia of monkeys [14]. For causal walking and the shifting of weight from one leg to the other, typical strain values were in the range of 100–400 μm/m. During peaks of vigorous jumping activity in cages, measured strains were as high as 1060 μm/m, representing a stress level of 200 kg. For a nominal 10-kg animal, that corresponds to 20 times the acceleration due to gravity. As many as 3–5 events/s were recorded; the onset or risetime of the largest strains, which were well within the range of the linear elastic response of bone, was 30–40 ms. In contrast, during restraint measurable strains in the tibia are infrequent and seldom exceed 100 μm/m. Hence, in a general way, bone loss in the lower extremities is related to a reduction of (a) strain normally associated with axial loads and bending moments, (b) pressure of the musculature against the periosteum, and (c) tension in the fibrous tendon insertions.

The techniques used supplemented each other in demonstrating differences in bones at the endosteal and subperiosteal surfaces, and in demonstrating intracortical changes that are characteristic of elevated states of bone resorption. Qualitatively, tomography shows a reduction of mineralized tissue per unit thickness of bone probably due to the presence of resorption cavities. Bone mass loss in the tibia and fibula appears to be regional.

In the present study, large changes were seen in the proximal tibia in the general area of the patellar tendon insertion; however, the radius and ulna were stable. The rib also appears to be unchanged. For example, in an earlier study (Hassing and Flora, personal communication), the morphometry of the rib was examined during a 7-month restraint. Achromysin, 20 mg/kg, i.v. was administered twice over a 5-week interval during the final phases of the test. The data shown in Table 1 were obtained by Hassing and Flora from 3 restrained monkeys and their corresponding cage controls. If restraint stimulated bone resorption in the cortex, one would expect cortical bone area to be decreased and cortical porosity to be increased. If restraint stimulated resorption at the endosteal surface, one would expect an increase in resorption surfaces, and possibly a decrease in surfaces with osteoid seams and fluorescent labels as well as a decrease in endosteal apposition rate. On the other hand, any effect on the width of the osteoid seams would suggest an effect on osteoid production or mineralization rate. The data shown in Table 1 are quite variable, although the average values indicate no systematic differences between controls and restrained animals. Thus it is likely that the rib is relatively stable and that there is only regional loss of skeletal mass during restraint.

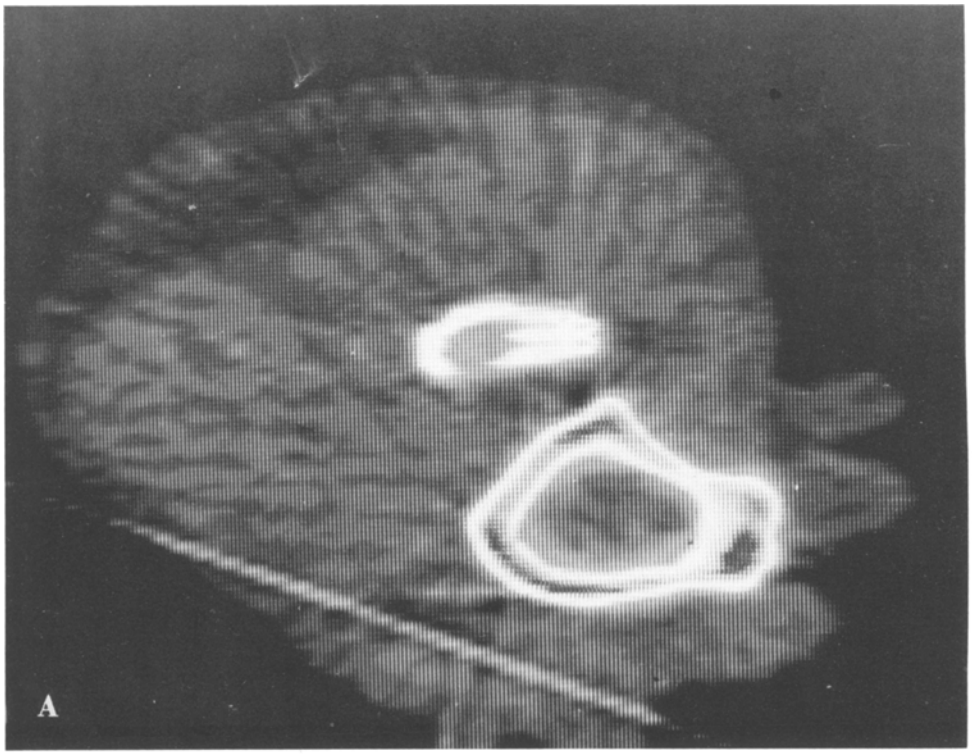
A

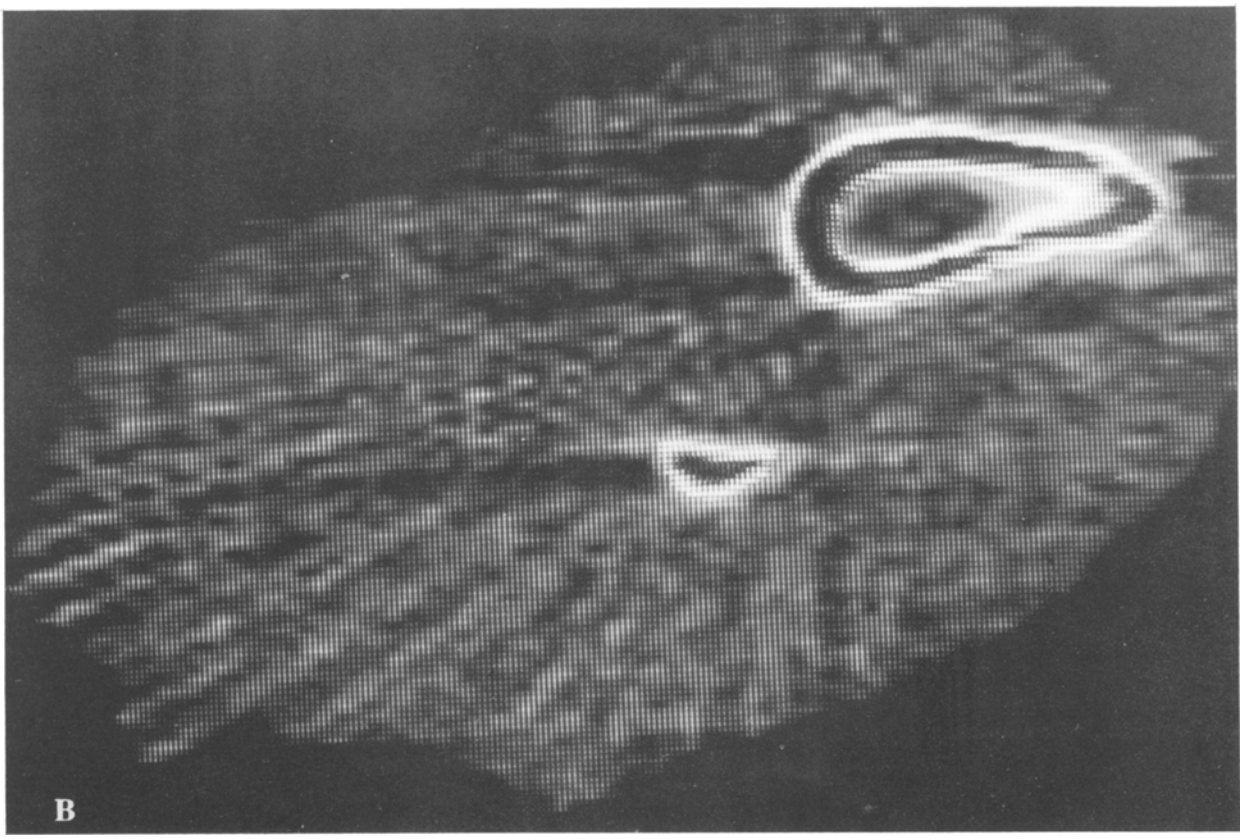
B

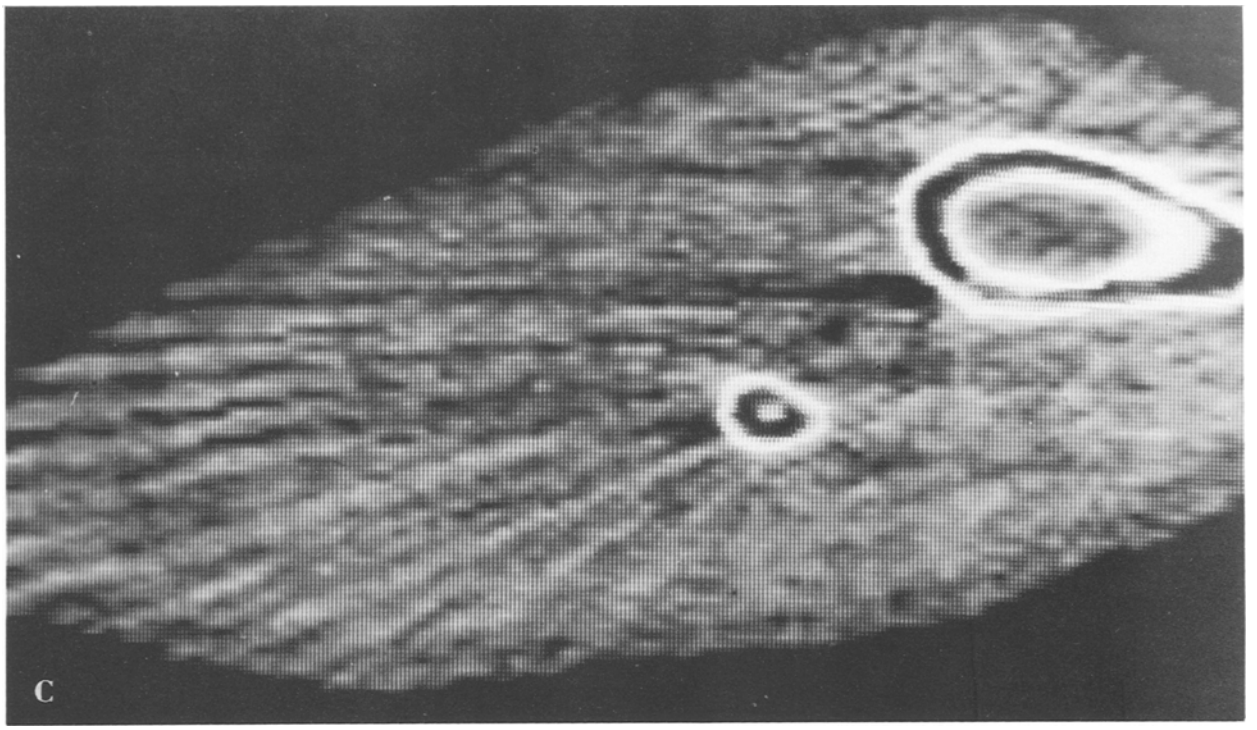

Fig. 5. Tomograms of the proximal left tibia of control animal No. 27 taken A 2.5 cm below the distal femur, B 2.8 cm below the femur, and C 3.1 cm below the femur. The anterior face of the tibia is shown to the right of the photo. The smaller fibula is shown adjacent to the posterior tibia. Muscle mass is shown surrounding both bones. The medullary space of the tibia is filled with marrow. Bone cortex consists of dense compact bone

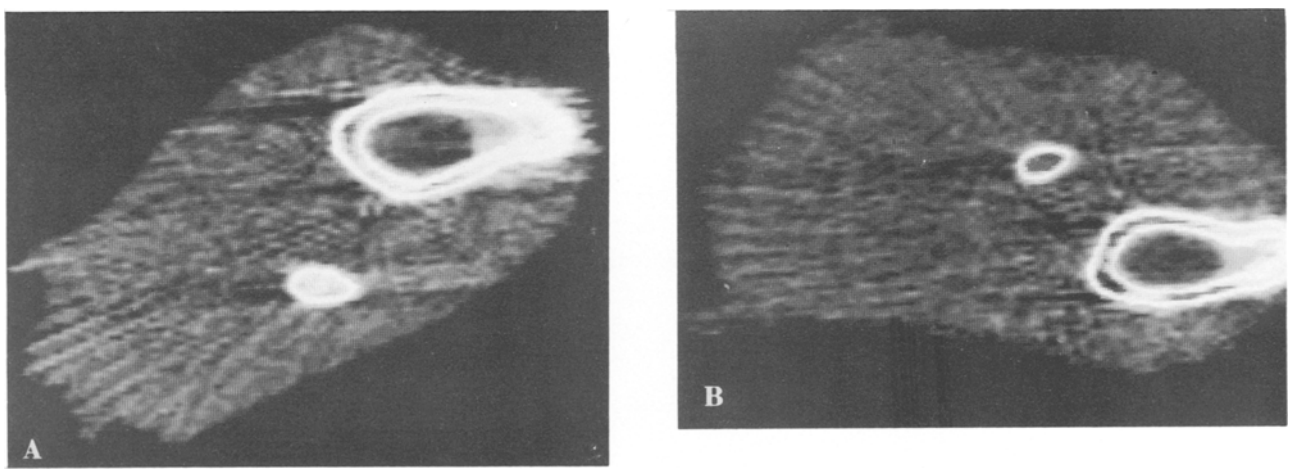

Fig. 6. A Cross section of left tibia of animal BO_3 after 5 months of restraint; taken 2.5 cm below the femur. The anterior tibia is shown at the right of the photo. Outline of trabecular bone is shown at the endosteal surface. There are discontinuities in the heavy cortical bone in the anterior face. B Cross section of the tibial tuberosity in animal BO_3 after 4 months of recovery showing mineralization in the posterior tibia.

Furthermore, the exchangeable calcium pool in the monkey is small. Studies with ^{47}Ca [15] indicate that the quantity of calcium distributed in mixing pools, as well as in the skeleton, is 0.8–1.0 g. Total skeletal calcium is about 200 g. Consequently, in our animals that showed increased bone resorption and high bone turnover, the activity of regional "hot spots" would involve only a fraction of exchangeable calcium and total body calcium. Overall, it would appear that there can be large losses constrained to certain skeletal areas, and involving a relatively small portion of total skeletal mass.

Failure to obtain tomograms sequentially throughout the study precludes evaluations of system-

Table 1. Bone morphometry data of the rib

Bone parameter	Restrained monkeys				Control monkeys			
	No. 6	No. 33	No. 35	$\bar{x}$	No. 30	No. 34	No. 37	$\bar{x}$
Total cortical area, mm^2	7.66	7.44	7.05	7.38	6.28	6.93	6.68	6.63
Cortical bone area, mm^2	7.26	6.45	6.44	6.72	5.95	6.24	6.21	6.13
Cortical porosity, mm^2	0.40	0.99	0.61	0.67	0.33	0.69	0.47	0.50
Number of resorption spaces in cortex per mm^2	0.41	0.47	0.20	0.36	0.62	0.16	0.16	0.31
% endosteal perimeter with resorption surface	18.5	5.3	2.3	8.7	8.5	6.1	15.5	10.0
% endosteal perimeter with osteoid seams	51.8	25.3	1.8	26.3	46.9	12.4	10.3	23.2
Width of Haversian osteoid seams, μm	8.18	7.84	7.36	7.79	7.56	7.64	11.44	8.88
Endosteal apposition rate, μm/day	0.21	0.23	0.13	0.19	0.18	0.11	0.22	0.17

From G. Hassing and L. Flora, Procter and Gamble Co.

atic trends in the data or an evaluation of individual differences. The main advantage of the use of tomography has been the demonstration of cross section anatomy. Tomography can demonstrate (a) the apparent crumbling erosion of cortical bone in the anterior tibia, and (b) resorption leading to endosteal widening, which is a criterion of high bone turnover states. Tomography can also demonstrate patterns of recovery and the location of new bone deposits, both of which could be useful adjuncts to histomorphologic evaluations concerning osteoblastic activity. However, neither tomography nor Norland bone mineral analysis clearly defines the individual cortical striations. Norland bone mineral provides only an integrated value of mineral, and is relatively insensitive to local changes. Nevertheless, the two techniques, along with X-rays, agree in demonstrating (a) a reduction of mineral content per unit length of bone, and (b) a reduction of mineral content per unit thickness of bone. Thus they demonstrate a clear osteopenia. Based on earlier results [9], we anticipate that the density and the modulus of the remaining bone are within normal limits.

The data indicate a local-regional uncoupling of bone formation/bone resorption during restraint with a relative increase in resorption rate. During recovery, osteoid tissue formation and mineralization appear to proceed at a slow rate. Thus there are probably several mechanisms involved with the sequence of events beginning with the induction of increased resorption rate during restraint to an apparently delayed restoration of bone during recovery.

The responses to a hypodynamic state could have serious consequences. For example, normally the outermost cortical fibers in the tibia are subjected to the greatest deformations in axial loading and bending. The present data show that there can be considerable losses of cortical bone, and therefore potentially a decrease in the average bending stiffness of the bone. Also, it is interesting to speculate whether the observed changes would compromise the collagenic Sharpey's fibers of the tendon insertion in the anterior tibia, or whether the erosion of cortical bone might facilitate local fracture initiation and crack propagation. Finally, it is possible that new bone formed during recovery has a relatively greater fraction of new osteons with a relatively large cavity area, and therefore with relatively less bone to resist stress.

To date, we have not developed quantitative data with tomography. Computations of the cross-sectional area of cortical bone and its distribution about the principal axes would provide useful information relative to the structural properties of the tibia.

Acknowledgments. We express our thanks to Mr. William Jackson for assistance in animal experimentation, and to Dr. Gordon Hassing and Mr. L. Flora of the Procter and Gamble Co. for the bone morphometry data.

References

1. Dietrick, J. E., Whedon, G. D., Shorr, E.: Effects of immobilization upon various metabolic and physiologic functions of normal men, Am. J. Med. 4:3–36, 1948
2. Donaldson, C. L., Hulley, S. B., Vogel, J. M., Hattner, R. S., Boyers, J. H., McMillan, D. G.: Effects of prolonged bed rest on bone mineral, Metabolism 19:1071–1084, 1970
3. Ascenzi, A., Bell, G. H.: Bone as a mechanical engineering

problem. In G. H. Bourne (ed.): The Biochemistry and Physiology of Bone, 2nd Ed., Vol. 1, pp. 311–352. Academic Press, New York, 1972
4. Saville, P. D., Smith, R.: Bone density, breaking force and leg muscle mass as functions of weight in bipedal rats, Am. J. Phys. Anthropol. **25**:35–39, 1966
5. Chamay, A., Tschantz, P.: Mechanical influences in bone remodelling. Experimental research on Wolff's Law, J. Biomech. **5**:173–180, 1972
6. Jones, H. H., Priest, J. D., Hayes, W. C., Tichenox, C. C., Nagel, D. A.: Humeral hypertrophy in response to exercise, J. Bone Joint Surg. **59-A**:204–209, 1977
7. Kazarian, L. E., von Gierke, H. E.: Bone loss as a result of immobilization and chelation: preliminary results in Macaca mulatta, Clin. Orthop. **65**:67–75, 1969
8. Young, D. R., Adachi, R. R., Howard, W. H.: Bone mineral losses during hypolinesis in primates (*M. nemestrina*). Abstract, 46th Annual Scientific Meeting, Aerospace Medical Association, San Francisco, April 28–May 1, 1975
9. Young, D. R., Howard, W. H., Cann, C., Steele, C. R.: Noninvasive measures of bone bending rigidity in the monkey (*M. nemestrina*), Calcif. Tissue Int. **27**:109–115, 1979
10. Howard, W. H., Parcher, J. W., Young, D. R.: Primate restraint system for studies of metabolic responses during recumbency, Lab. Animal Sci. **21**:112–117, 1971
11. Rüegsegger, P., Niederer, P., Anliker, M.: An extension of classical bone measurements, Ann. Biomed. Eng. **2**:194–205, 1974
12. Rüegsegger, P., Elsasser, V., Anliker, M., Gnehm, H., Kind, H., Prader, A.: Quantification of bone mineralization using computed tomography, Radiology **121**:93–97, 1976
13. Andersson, S. M., Nilson, B. E.: Fracture—and immobilization osteoporosis in man, Calcif. Tissue Int. [Suppl.] **24** 1977 (abstr.)
14. Young, D. R., Howard, W. H., Orne, D.: *In vivo* bone strain telemetry in monkeys (*M. nemestrina*), J. Biomech. Eng. **99**:104–109, 1977
15. Cann, C., Young, D. R.: Bone formation rate in experimental disuse osteoporosis in monkeys (*M. nemestrina*), Physiologist **19(3)**:147, 1976 (abstr.)